NUMERICAL SIMULATION OF FLOW AND HEAT TRANSFER AROUND VERTICAL CYLINDER SUBMERGED IN WATER

Ahmed Ramadan*, ahmed.ramadan@northumbria.ac.uk
Reaz Hasan, reaz.hasan@northumbria.ac.uk
Roger Penlington, r.penlington@northumbria.ac.uk

Northumbria University at Newcastle, Department of Mechanical and Construction Engineering, Ellison Place, Newcastle upon Tyne, NE1 8ST, UK

ABSTRACT

Natural convection flows around submerged heated cylinders have gained attention in recent years due to their use in many engineering applications such as flow around tubes and rods (as in nuclear reactors and spent fuel cooling ponds). The purpose of this paper is to establish the modelling strategy for simulating natural convection heat transfer and flow around vertically positioned cylinders submerged in a water tank heated with a constant heat flux. The simulations were conducted for cylinders having different diameters which varied from 10 mm to 165 mm. The problem involved flow transition from laminar to turbulent within the boundary layer as the maximum Rayleigh number based on the cylinder length reached a magnitude of the order of 10^{14}. The outcomes of these calculations were validated against published experimental data. The comparisons were made in terms of heat transfer coefficient and Rayleigh number which showed good agreement between predictions and experimental results.

The predicted results showed sensitivity to various eddy viscosity models and the final results were obtained with SST model. Another important point that emerged from the study was that the specification of a suitable evaporation boundary condition at the top (water) surface was very critical. The treatment of evaporation from the top surface is discussed in detail which was also successfully incorporated in the methodology. We believe that the results obtained from our study will be useful for modelling flow in situations where a large number of heated cylinders are involved.

INTRODUCTION

In recent years, natural convection heat transfer around vertical cylinders has gained increased attention owning to its significant applications, specially, in the nuclear applications starting from the reactor core to the nuclear waste management. For the purpose of this research we have practically focused on the waste management applications (Hasan et al., 2015). The Spent Nuclear Fuel (SNF), nuclear waste, needs to be submerged under water in cooling ponds for several years until became less radioactive.

SNF cooling ponds, in principle, based on two phenomenon to get rid of the decay heat released from the fuel racks. First is natural convection phenomenon between the fuel racks and the surrounding water. The second mechanism is via the complex phenomenon of evaporation into atmosphere from the free water surface which represents the major component of the heat loss from such ponds. These two fundamental phenomenon will be discussed in detailed in the following sections.

Establishing a methodology for modelling submerged vertical cylinders will allow more understanding of the flow behaviour in such situations. The well-known Computational Fluid Dynamics (CFD) methodology will be used in this study and the general methodology can be found in many textbooks such as (Versteeg and Malalasekera, 2007).

A rule of thumb is that most of numerical methodologies need to be validated against reliable experimental data to give the confidence of the obtained results. After reviewing the literature we found few experimental work been conducted on heated vertical cylinders submerged in water which can be used to validate our numerical methodology.

(Kimura et al., 2004) have experimentally investigated the heat transfer around heated vertical cylinder submerged in a water tank as shown in Fig. 1. The cylinder was supplied with constant heat flux. A unique aspect of the work of (Kimura et al., 2004) was that they have studied the effect of the diameter to height (*D/L*) ratio of the cylinder on the heat transfer characteristics where the diameter was varied from 10 to 165 mm. The study shows that increasing the cylinder diameter results in shifting the onset of transition vertically upward direction and the heat transfer coefficient has considerably enhanced with reducing the diameter.

(Arshad et al., 2011) have reported an experimental work of natural convection heat transfer from a 3 x 3 array of thin vertical cylinders. The cylinder assembly was submerged in a large water tank where all cylinders were heated with uniform heat flux. The results showed that the temperature distribution on the cylinders surfaces is gradually increased in the axial direction until the flow transition from laminar to turbulent the temperature starts to fall down enhancing the heat transfer. As outcome of this study, they proposed empirical correlations for an assembly of cylinders in terms of Nusselt and Rayleigh numbers.

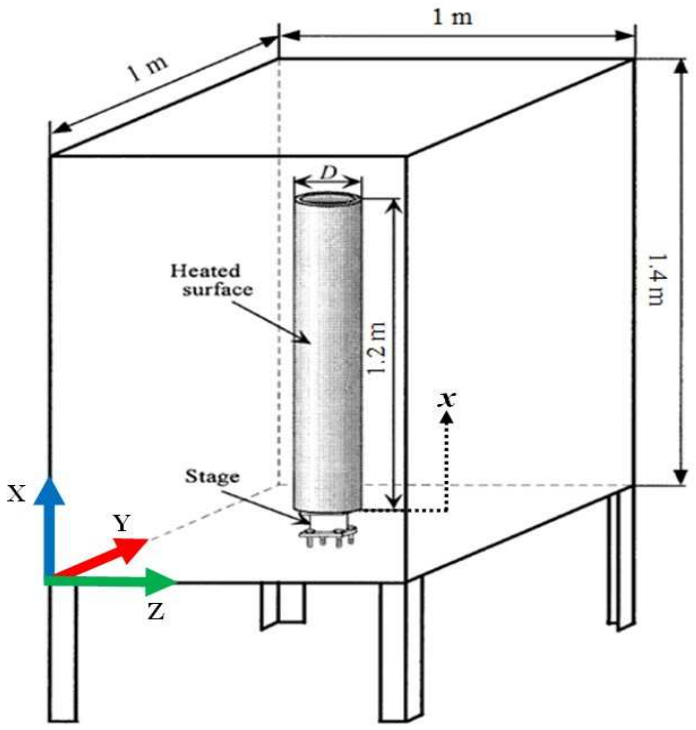

Fig. **1**. Sketch of the experimental apparatus (Kimura et al., 2004).

From the experimental work found in the literature we have carefully chosen the experiment conducted by (Kimura et al., 2004) to validate our modelling methodology with their data. This experiment was selected for few reasons as listed below.

- The heat transfer medium is water.
- The position and shape of the cylinder
- The cylinder is heated with uniform heat flux which is similar to the situation in the cooling ponds.
- Allow to examine the effect of cylinder diameter on the heat transfer characteristics
- Water top surface is exposed to atmosphere to allow for evaporation to take place.

The knowledge gained from this validation exercise will be partially applied in future to produce a valid numerical model of the SNF cooling pond. In addition, this validation exercise will provide a baseline for modelling flow in similar situation.

NATURAL CONVECTION HEAT TRANSFER

When a heated body is immersed in a quiescent fluid, a natural circulation current is induced as a result of temperature gradient. This is happening due to the fact that the density of the fluid is highly dependent on temperature so that the hot fluid tends to move upward exchanging positions with the relatively colder fluid. The effect of natural convection may be neglected in some occasions when forced convection is introduced. The dimensionless relations which govern natural convection phenomenon, when uniform heat flux is provided, are modified Grashof number, Gr_L^*, modified Rayleigh number, Ra_L^*, and Nusselt number, Nu_L. These numbers can be defined as follows:

$$Gr_L^* = \frac{g\beta q_w^{\bullet} L^4}{k\nu^2} \tag{1}$$

$$Ra_L^* = Gr_L^* \,\mathrm{Pr} = \frac{g\beta q_w^{\bullet} L^4}{k\alpha\nu} \tag{2}$$

$$Nu_L = \frac{hL}{k} \tag{3}$$

where L is the length of the cylinder, and h is the convective heat transfer coefficient an calculated according to the following equation:

$$h = \frac{q_w^{\bullet}}{T_w - T_b} \tag{4}$$

HEAT LOSS FROM THE TOP SURFACE

The heat loss from the free water surface takes place by three different mechanisms; evaporation, convection, and radiation. The treatment of each mechanism is explained in the following sections. However, the total heat flux from the free water surface can be considered as follows:

$$q_{total}^{\bullet} = q_{evap}^{\bullet} + q_{conv}^{\bullet} + q_{rad}^{\bullet} \tag{5}$$

Evaporation Heat Loss

Given that the top surface of the water is exposed to the atmospheric air, it is important to understand the mechanism of evaporation to be able to specify the appropriate boundary condition in the numerical model.

Evaporation is the net mass loss from water surface as a result of phase change from a liquid to a vapour. Water vapour is in constant motion, moving back and forth from the free water surface. Evaporation takes place when the leaving molecules are more than entering. This process is associated with large amount of energy which is required to break the hydrogen bonds between the molecules of water allowing molecules to escape from the water surface. There are three drivers of the evaporation process and are listed below (Silberberg, 2006).

- The supplied heat energy which increases the kinetic energy of the water molecules.
- Diffusion of water vapour from the free water surface to the surrounding humid air.
- Transport of water vapour within the layers of the atmosphere away from the water surface.

Diffusion occurs when the fluid phase changes from liquid to gaseous phase, which takes place at a very thin boundary layer just above the free water surface (Thompson, 1998). The result is that the moisture moves from the regions of high concentrations to lower concentrations in the form of vapour (McQuiston et al., 2005). This thin boundary layer can be assumed as air fully saturated by water vapour. However, evaporation rate is mainly affected by the velocity of surrounding air, water and air temperatures, water surface area, and humidity (Vinnichenko et al., 2011, Magin and Randall, 1960).

Evaporation can occur due to two mechanisms, first, is free evaporation (when the surrounding air is at rest) because of the difference in moisture concentration between the thin layer of the air directly above the water surface and the surrounding air. The second mechanism is the forced evaporation as a result of air flow across the free water surface (Shaw, 1998). There are many approaches to estimate the evaporation rate; the most commonly is through an experimental measurement or by using the well-known similarity theory. This theory assumes the complete analogy between convective heat and mass transfer under some conditions.

(Bower and Saylor, 2009) have experimentally investigated the natural convection driven evaporation. Sixteen different water tanks having different sizes were used where measurements of relevant temperature and relative humidity were collected. They have developed a power law correlation between Rayleigh number and Sherwood number for evaporation. They found that the value of the exponent of the power law correlation is very close to 1/3 which is similar to the exponents of *Nu – Ra* power law correlations for convective heat transfer in many studies.

(Jodat et al., 2013) have experimentally studied the ability of similarity theory to estimate the water evaporation rate. The study has considered free, forced, and mixed convection regimes. They have considered in their study water temperatures ranged between 20 to 55 ^{o}C and the air average velocities varied from 0.05 to 4 m/s. For the natural convection regime, the similarity theory has well predicted the evaporation rate; however, in the combined regime the similarity theory was not able to predict the nonlinear behaviour. In the forced convection regime, the similarity theory underestimated the evaporation rate. The outcomes of this investigation were summarised in a new correlation for the mixed convection to enhance the results for this regime.

In the present study, we have assumed that the surrounding humid air is quiescent so that the evaporation from the free water surface can only occur naturally. Hence, the similarity theory between heat and mass transfer can be used for the purpose of this validation work. The dimensionless mass transfer coefficient, Sherwood number, is defined as the following power law correlation Eq. (6) (Cengel, 2003).

$$Sh = 0.15\left(Gr_m Sc\right)^{1/3} \tag{6}$$

where Sc and Gr_m are the Schmidt and Grashof numbers for mass transfer, respectively, and can be defined as:

$$Sc = \frac{\nu}{D_{H_2O,air}} \tag{7}$$

$$Gr_m = \frac{g\left(\rho_\infty - \rho_s\right)}{D_{H_2O,air}} \tag{8}$$

Therefore, the mass transfer coefficient can be calculated from the following equation:

$$Sh = \frac{h_m L_c}{\rho D_{H_2O,air}} \tag{9}$$

where, the characteristic length, L_c, is considered as follows:

$$L_c = \frac{Area}{Perimeter} \tag{10}$$

and $D_{H_2O,Air}$ is the mass diffusivity of water vapour in air at the average temperature and can be evaluated from the following expression:

$$D_{H_2O,Air} = 1.87 \times 10^{-10} \frac{T^{2.072}}{P} \tag{11}$$

Then the evaporation mass flux, $m^{\bullet}$, can be found from:

$$m_e^{\bullet} = h_m \left(\rho_{v,s} - \rho_{v,\infty} \right) \tag{12}$$

Finally, the heat flux due to evaporation can be calculated as follows:

$$q_{evap}^{\bullet} = m_e^{\bullet} h_{fg} \tag{13}$$

where h_{fg} is the latent heat of vaporisation.

Convection and radiation heat loss

The heat loss form the water top surface by the mean of natural convection and radiation is less significant than the evaporation heat loss. However, it cannot be ignored as the water bulk and surface temperatures are very sensitive to the boundary condition at the top surface.

The heat loss by convection from the free water surface to the atmosphere can be treated as a horizontal plate and the correlation in Eq. (14) can be used to evaluate the convective heat transfer coefficient which is analogy with the mass transfer correlation as shown in Eq. (6).

$$Nu = 0.15 \left(Gr \, \mathrm{Pr} \right)^{1/3} \tag{14}$$

$$Nu = \frac{h_{conv} L_c}{k} \tag{15}$$

Then, the convective heat flux can be calculated from the following equation:

$$q_{conv}^{\bullet} = h_{conv} \left(T_s - T_{\infty} \right) \tag{16}$$

The radiation heat flux can be found from:

$$q_{rad}^{\bullet} = \varepsilon \sigma \left(T_s^4 - T_{surr}^4 \right) \tag{17}$$

NUMERICAL SIMULATION

The experiment conducted by (Kimura et al., 2004) was used to validate our numerical methodology. A sketch of the experimental apparatus is shown in Fig 1. The vertical cylinder as shown in figure is heated with constant heat flux with value of 5000 W/m^2 where the surrounding water temperature was initially at ambient temperature. The simulations were conducted for cylinders having diameters 10 mm, 26 mm and 165 mm. The problem involved flow transition from laminar to turbulent within the boundary layer as the maximum modified Rayleigh number based on the cylinder length reached a magnitude of the order of 10^{14}. Due to the symmetry in the geometry of the experimental apparatus, only one quarter of the geometry is considered for all the simulation cases to reduce the computational time.

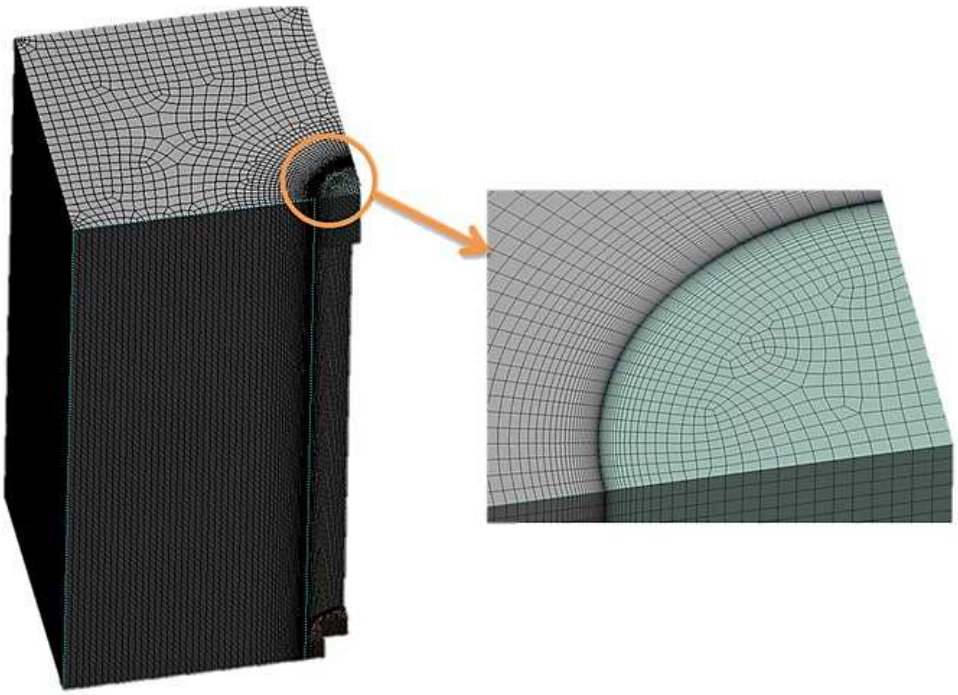

Fig. 2. Grid distribution of the computational domain for Kimura et al. experiment.

The computational grid shown in Fig. 2 was constructed mostly with hexahedral mesh to generate number of cells around 0.5 million. Inflation was used at the cylinder surface to control the y^+ value and the wall normal expansion ratio (maximum of 1.1). During the simulation the y^+ value was kept in range of 0.25 to 0.9 which is fine enough to capture the flow transition from laminar to turbulent (Fluent, 2014).

Various eddy viscosity turbulence models were tested to find out which of these models has the capability to capture the transition behaviour of the flow. Transition shear stress transport (SST) turbulence model (Menter et al., 2006) was found to lead to satisfactory results providing that y^+ at the cylinder surface was kept within the recommended value (0.001 to unity).

In order to model the buoyancy driven flow, gravity was specified with value of 9.81 m/s^2 downward. Besides, all the properties of water were considered to be temperature dependent. All the physical properties of water follow the relation described in Eq. (18), except the thermal expansion coefficient which can be evaluated from Eq. (19) (Arshad et al., 2011).

$$\varphi = A + BT_f + CT_f^2 + DT_f^3 \tag{18}$$

$$\beta = -\tfrac{1}{\rho}(A + 2BT_f + 3CT_f^2) \tag{19}$$

where φ represents all the physical properties of water (ρ, C_p, k, μ), except the thermal expansion coefficient (β). T_f is the film temperature. *A, B, C and D* are thermodynamics constant and their values are summarised in Table 1.

Table 1. Thermodynamic constants for physical properties of water (Arshad et al., 2011).

Property / thermodynamics constant	*A*	*B*	*C*	*D*
Density (ρ) (Kg/m^3)	223.127	6.7678	-1.8538 x 10^{-2}	1.522 x 10^{-5}
Specific heat (C_p) (J/Kg K)	5021.28	-5.4571	8.842 x 10^{-3}	-
Thermal conductivity (k)(W/m K)	-5.084 x 10^{-1}	6 x 10^{-3}	-7.565 x 10^{-6}	-
Viscosity (μ) (Pa.s)	6.3225 x 10^{-2}	-5.1485 x 10^{-4}	1.415 x 10^{-6}	-1.306 x 10^{-9}
Thermal expansion coefficient (β) (1/K)	6.7678	-1.8538 x 10^{-2}	1.522 x 10^{-5}	-

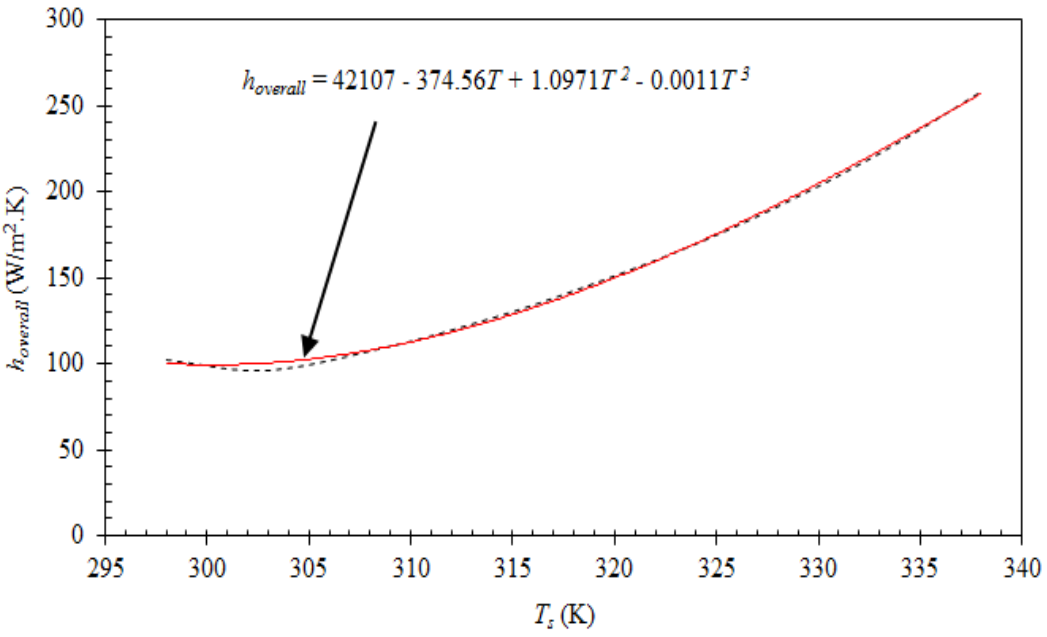

Fig. 3. The overall heat transfer coefficient corresponding to the water surface temperature.

The evaporation heat flux from the water free surface can be obtained by applying the similarity theory at a wide range of water surface temperatures Eq. (6 to 13). In the same way, the convective and radiative heat fluxes can be calculated using Eq. (16) and Eq. (17), respectively. In the previous calculations, the humid air conditions were considered to be at a temperature of 295 K and relative humidity of 70%. In addition, the air properties (k, υ, α, Pr) were estimated at the average temperature (between air and water surface temperatures).

Now, the values for the total heat flux may obtain from Eq. (5) and then the results can be converted to overall heat transfer coefficient, $h_{overall}$. After evaluating the overall heat transfer coefficient, $h_{overall}$, at the free water surface under different water surface temperatures, these data can be plotted in form of $h_{overall}$ against the water surface temperature, T_s, as shown in Fig. 3, and the best fit curve polynomial correlation is obtained Eq. (20).

In order to utilise the new correlation for the overall heat transfer coefficient Eq. (20), a user-defined-function (UDF) was written and compiled to the Fluent solver (Fluent, 2014).

$$h_{overall} = 42107 - 374.56T + 1.0971T^2 - 0.0011T^3 \tag{20}$$

The simulations were conducted until the steady state was reached for the three cases. The commercial CFD package of ANSYS Fluent 15.0 was used to perform these calculations, where the continuity, momentum and energy equations were solved. All the conservation equations were solved with second order upwind scheme, except the continuity equation which used PRESTO!. The calculations were performed with residual criterion of 10^{-4} on an i7- 3770 CPU @ 3.40 GHz 4 cores machine. A typical computation needed 12 hours.

RESULTS AND DISCUSSION

The results obtained from the simulations were processed and displayed in the form of surface temperature, heat transfer coefficient along the cylinder surface, and Nu_x vs. Ra_x*.

Surface Temperature Visualisation

Figure 4 shows the temperature distributions along the surface of the cylinder for three different diameters. The colours shown in this visualisation are indicating as follows, black (low temperature), light grey (moderate temperature), and dark grey (high temperature). It can be clearly seen from the photos in Fig. 4 that the predicted results show good agreement with those obtained from the experiment. The lowest temperatures were recorded at the bottom of the cylinder where the temperature values keep increasing in the vertical upward direction up to the separation point where the transition from laminar to turbulent takes place.

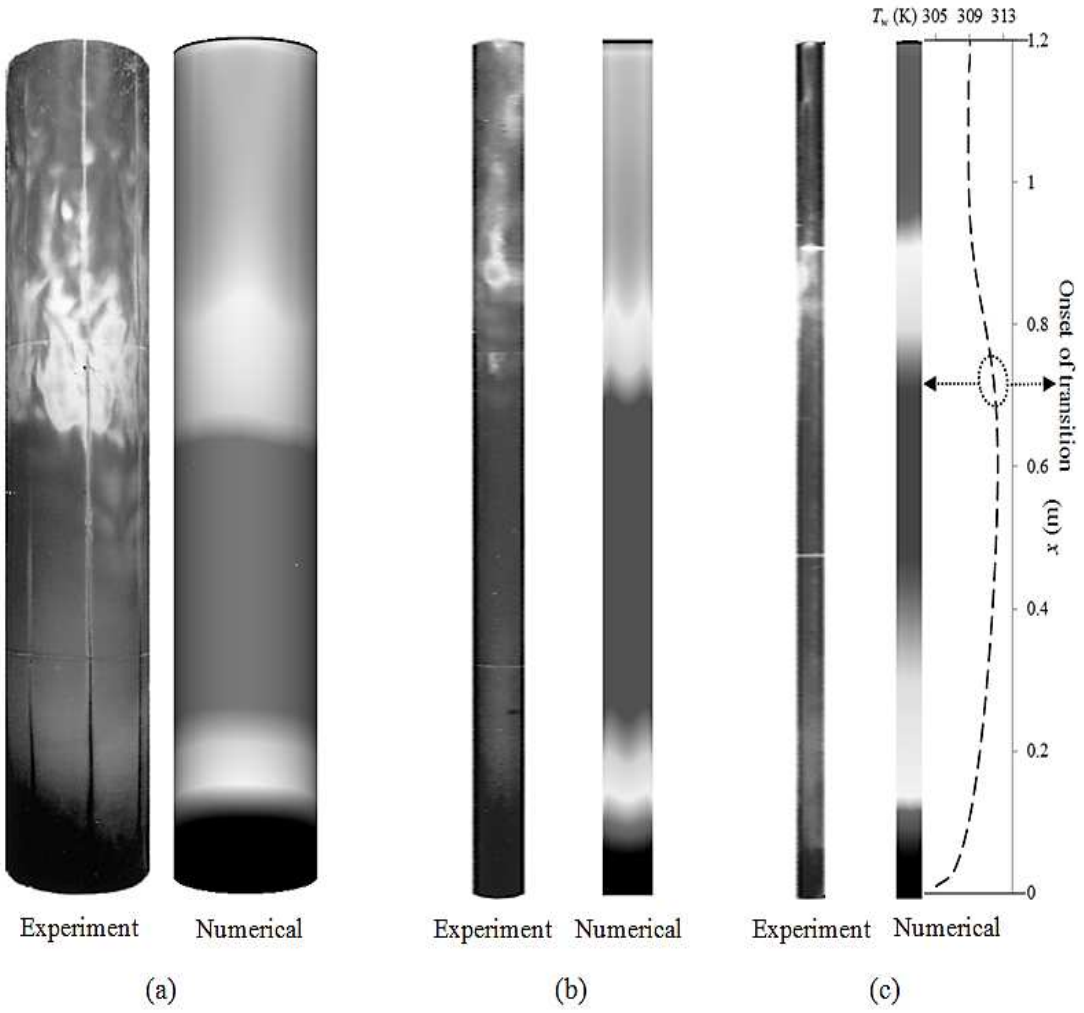

Fig. 4. Temperature distribution along the cylinder surface. (a) D = 165 mm, (b) D = 26 mm, and (c) D = 10 mm.

The observed temperature gradient in the bottom part of the cylinders is due to the effect of the buoyancy driven flow within the boundary layer. This flow behaviour should be more pronounced with increasing the axial distance

According to the visualisation photos in Fig. 4, the onset of transition to turbulence keeps shifting in the vertical upward direction with decreasing the diameter of the cylinder and this is due to the increase of the curvature effect. When the boundary layer becomes turbulent, the temperature starts to decrease gradually in the vertical upward direction.

Heat Transfer Characteristics

Figure 5 shows the comparisons of heat transfer coefficient between the predicted results and experimental data (Kimura et al., 2004). Overall the comparisons show a good agreement. However, minor differences can be observed which is probably due to uncertainty in geometry and the validity of the top surface heat loss correlation where the discrepancy is more pronounced. It can be clearly seen in Fig 5 that the heat transfer coefficient gradually falls with increasing height of the cylinder up to the point where the flow transition from laminar to turbulence takes place. After that the flow became fully turbulent, at the top region of the cylinder, resulting in enhancement of the heat transfer.

As the water properties are considered to be temperature dependent, any change in the temperature will directly affect the flow and heat transfer characteristics. Figure 6 displays the viscosity and the thermal conductivity of water within the boundary layer in the vertical upward direction. The increase of surface temperature, vertically upward direction, decreases the dynamic viscosity, μ, and increases the thermal conductivity, k.

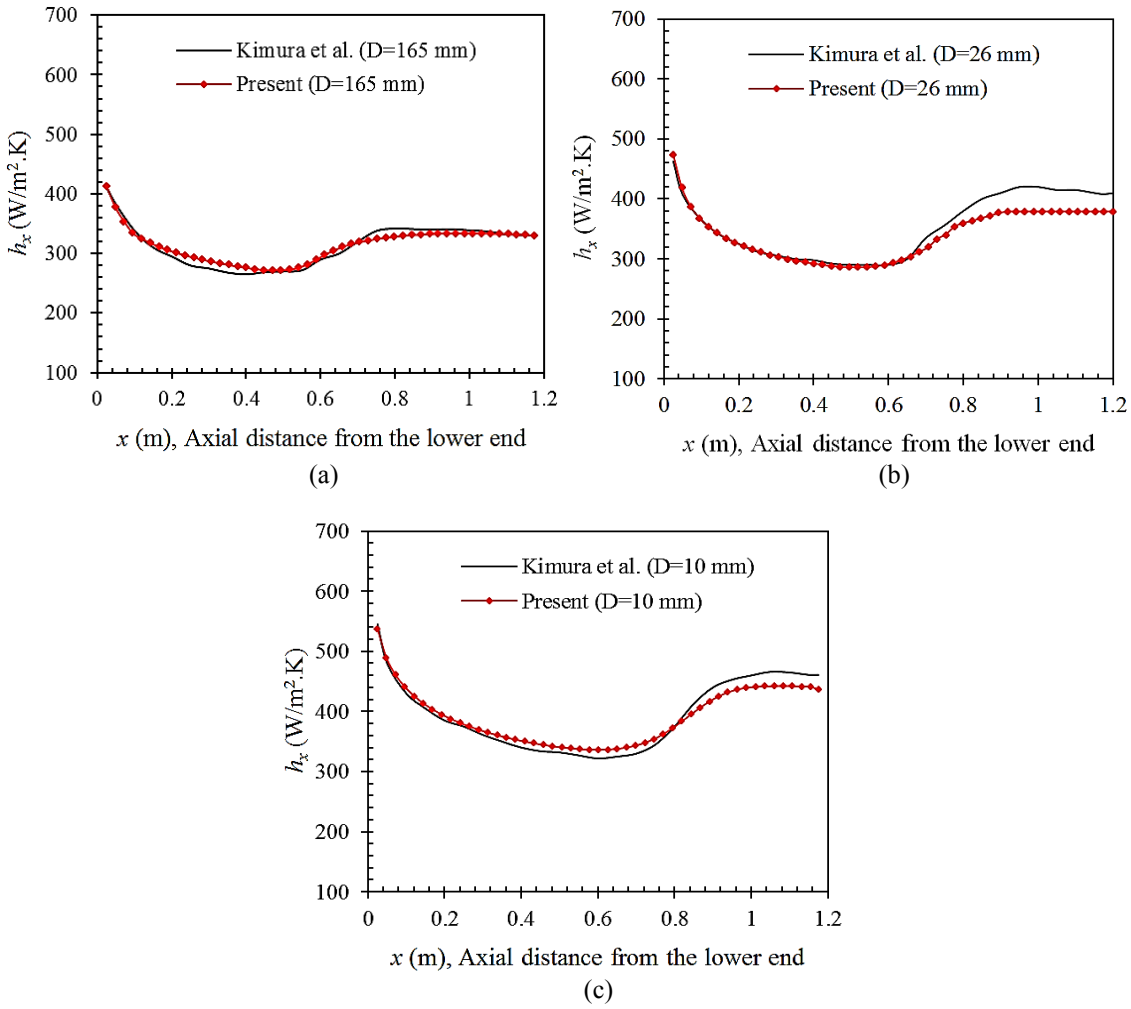

Fig. 5. Comparisons of local heat transfer coefficient between the present work and data for Kimura et al. [xx] for different diameters (a) D =165 mm, (b) D =26 mm, and (c) D =10 mm.

At the peak of the surface temperature, the viscosity is at its lowest value which in turn increases the Rayleigh number transforming the flow to be fully turbulent in this region. Meanwhile, the thermal conductivity decreases due to the high temperature offering higher resistance to the heat transfer. After the flow is fully turbulent, the turbulence activities lead to reducing the temperature in the top region of the cylinder. Accordingly, the thermal conductivity increases offering less resistance to heat transfer. In general, the heat transfer coefficient is enhanced more for smaller cylinder diameters.

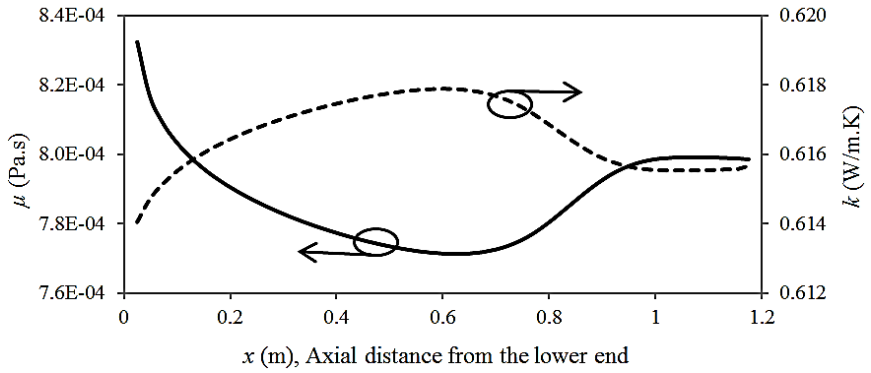

Fig. 6. Dynamic viscosity and thermal conductivity distributions of the water within the boundary layer along the cylinder length having a diameter of D = 10 mm.

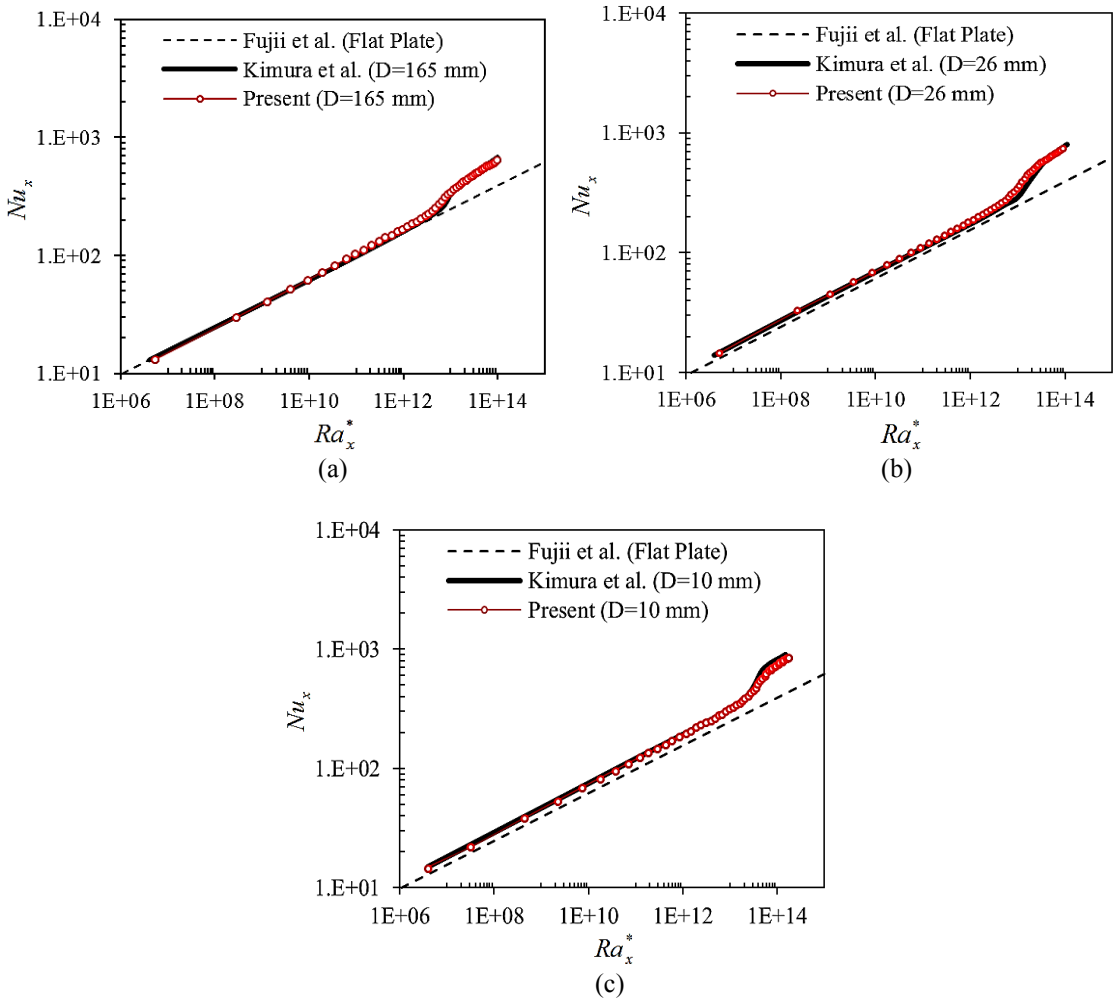

Fig. 7. Comparisons of local Nusselt number between the present work and data for vertical cylinder by Kimura et al. (Kimura et al., 2004) and vertical plate by Fujii et al. (Fujii et al., 1970) for different diameters (a) D =165 mm, (b) D =26 mm, and (c) D =10 mm.

The plots of the non-dimensional local Nusselt number, Nu_x, against the local modified Rayleigh number, Ra_x*, are shown in Fig 7. For the biggest diameter, 165 mm, the predicted data agreed well with the proposed data by Fujii et al. (Fujii et al., 1970) for vertical flat plate in the laminar regime shown in Fig. 7 (a). These data match with those obtained by (Kimura et al., 2004) over the laminar region as well as the turbulent region.

Figures 7 (b) & (c) show a comparison for the smaller diameters, 26 mm and 10 mm, respectively. Overall, the current data are in good agreement with data reported by (Kimura et al., 2004), however, there is a deviation from (Fujii et al., 1970) and this deviation increases for the smallest diameter, 10 mm. The reason for this discrepancy is due to the high curvature of cylinder.

CONCLUSIONS

The modelling methodology of heated vertical cylinder submerged in a water tank was established and the validation work was successful. Numerical simulation was conducted and the obtained data were validated against the experimental data reported by (Kimura et al., 2004). The CFD model was able to predict the temperature distribution along the heated surface of the cylinder and locating the flow separation point with good accuracy. Also, it appears that the treatment of the boundary condition at the free water surface is capable to evaluate the total heat loss due to evaporation, convection, and radiation. The discrepancies were probably due to uncertainties in geometry specifications.

The presented methodology provides a baseline for modelling flows in similar situations and can be further extended to model the SNF cooling pond and other situations where a large number of vertical cylinders are used.

NOMENCLATURE

Symbols

D	diameter of the cylinder (m)
$D_{H_2O,Air}$	mass diffusivity of water vapour in air
g	acceleration of gravity (m/s^2)
$Gr*$	modified Grashof number (dimensionless)
h	heat transfer coefficient (W/m^2·K)
k	thermal conductivity (W/m·K)
L	length (m)
$m_e^{\bullet}$	evaporation mass flux Kg/s.m^2
Nu	Nusselt number (dimensionless)
P	pressure
Pr	Prandtl number (dimensionless)
$q^{\bullet}$	heat flux (W/m^2)
Ra	Rayleigh number (dimensionless)
Sc	Schmidt number (dimensionless)
Sh	Sherwood number (dimensionless)
T	Temperature (K)
x	axial coordinate (m)

Greek Symbols

α	thermal diffusivity (m^2/s)
β	coefficient of thermal expansion (1/K)
ε	water emissivity
μ	dynamic viscosity (Pa.s)
v	kinematics viscosity (m^2/s)
ρ	density (kg/m^3)
σ	Stefan Boltzmann constant

Subscript

b	bulk
c	characteristic
$conv$	convective heat transfer
$evap$	evaporation heat transfer
m	mass transfer
rad	radiative heat transfer
s	surface
∞	ambient
$surr$	surrounding conditions
t	total
v,s	vapour at surface conditions
v,∞	vapour at ambient conditions
w	wall
x	local value

REFERENCES

ARSHAD, M., INAYAT, M. H. & CHUGHTAI, I. R. 2011. Experimental study of natural convection heat transfer from an enclosed assembly of thin vertical cylinders. *Applied Thermal Engineering,* 31**,** 20-27.

BOWER, S. & SAYLOR, J. 2009. A study of the Sherwood–Rayleigh relation for water undergoing natural convection-driven evaporation. *International Journal of Heat and Mass Transfer,* 52**,** 3055-3063.

CENGEL, Y. 2003. *Heat Transfer A Practical Approach, WCB McGraw-Hill*.

FLUENT, A. 2014. Theory and user's guide. *Ansys Corporation*.

FUJII, T., TAKEUCHI, M., FUJII, M., SUZAKI, K. & UEHARA, H. 1970. Experiments on natural-convection heat transfer from the outer surface of a vertical cylinder to liquids. *International Journal of Heat and Mass Transfer,* 13**,** 753-787.

HASAN, R., TUDOR, J. & RAMADAN, A. Modelling of Flow and Heat Transfer in Spent Fuel Cooling Ponds. Proceedings of the International Congress on Advances in Nuclear Power Plants 2015 2015. Nice, France.

JODAT, A., MOGHIMAN, M. & RAD, E. Y. 2013. An Experimental Study of the Ability of Similarity Theory to predict Water Evaporation Rate for Different Convection Regimes. *Arabian Journal for Science and Engineering,* 38**,** 3505-3513.

KIMURA, F., TACHIBANA, T., KITAMURA, K. & HOSOKAWA, T. 2004. Fluid flow and heat transfer of natural convection around heated vertical cylinders (effect of cylinder diameter). *JSME International Journal Series B Fluids and Thermal Engineering,* 47**,** 156-161.

MAGIN, G. B. & RANDALL, L. E. 1960. *Review of literature on evaporation suppression*, US Government Printing Office.

MCQUISTON, F. C., PARKER, J. D. & SPITLER, J. D. 2005. *Heating, ventilating, and air conditioning: analysis and design,* Chichester, Wiley.

MENTER, F., LANGTRY, R. & VÖLKER, S. 2006. Transition modelling for general purpose CFD codes. *Flow, Turbulence and Combustion,* 77**,** 277-303.

SHAW, E. 1998. Hydrology in practice 3rd ed. *Stanley Thornes Pub, UK pp569*.

SILBERBERG, M. S. 2006. *Chemistry: The Molecular Nature of Matter and Change*, McGraw-Hill.

THOMPSON, R. D. 1998. *Atmospheric processes and systems*, Psychology Press.

VERSTEEG, H. K. & MALALASEKERA, W. 2007. *An introduction to computational fluid dynamics: the finite volume method*, Pearson Education.

VINNICHENKO, N. A., UVAROV, A. V., VETUKOV, D. A. & PLAKSINA, Y. Y. 2011. Direct computation of evaporation rate at the surface of swimming pool.